Bioorganic Chemistry 54 (2014) 60–67

Contents lists available at ScienceDirect

Bioorganic Chemistry

journal homepage: www.elsevier.com/locate/bioorg

Cytotoxic benzophenone and triterpene from *Garcinia hombroniana*

Nargis Jamila [a], Melati Khairuddean [a,*], Nik Soriani Yaacob [b], Nik Nur Syazni Nik Mohamed Kamal [b], Hasnah Osman [a], Sadiq Noor Khan [c], Naeem Khan [d]

[a] School of Chemical Sciences, Universiti Sains Malaysia, 11800 Minden, Penang, Malaysia
[b] Department of Chemical Pathology, School of Medical Sciences, Universiti Sains Malaysia, 16150 Kubang Kerian, Kelantan, Malaysia
[c] Department of Medical Lab Technology, University of Haripur, 22060 Haripur, Khyber Pakhtunkhwa, Pakistan
[d] Department of Chemistry, Kohat University of Science and Technology, Kohat, 26000 Kohat, Khyber Pakhtunkhwa, Pakistan

ARTICLE INFO

Article history:
Received 17 February 2014
Available online 23 April 2014

Keywords:
Garcinia hombroniana
Bark
Benzophenones
Triterpenes
Cytotoxicity
Antioxidant activities

ABSTRACT

Garcinia hombroniana (seashore mangosteen) in Malaysia is used to treat itching and as a protective medicine after child birth. This study was aimed to investigate the bioactive chemical constituents of the bark of *G. hombroniana*. Ethyl acetate and dichloromethane extracts of *G. hombroniana* yielded two new (**1**, **9**) and thirteen known compounds which were characterized by the spectral techniques of NMR, UV, IR and EI/ESI-MS, and identified as; 2,3′,4,5′-tetrahydroxy-6-methoxybenzophenone (**1**), 2,3′,4,4′-tetrahydroxy-6-methoxybenzophenone (**2**), 2,3′,4,6-tetrahydroxybenzophenone (**3**), 1,3,6,7-tetrahydroxyxanthone (**4**), 3,3′,4′,5,7-pentahydroxyflavone (**5**), 3,3′,5,5′,7-pentahydroxyflavanone (**6**), 3,3′,4′,5,5′,7-hexahydroxyflavone (**7**), 4′,5,7-trihydroxyflavanone-7-rutinoside (**8**), 18(13 → 17)-abeo-3β-acetoxy-9α,13β-lanost-24*E*-en-26-oic acid (**9**), garcihombronane B (**10**), garcihombronane D (**11**), friedelan-3-one (**12**), lupeol (**13**), stigmasterol (**14**) and stigmasterol glucoside (**15**). In the *in vitro* cytotoxicity against MCF-7, DBTRG, U2OS and PC-3 cell lines, compounds **1** and **9** displayed good cytotoxic effects against DBTRG cancer cell lines. Compounds **1**–**8** were also found to possess significant antioxidant activities. Owing to these properties, this study can be further extended to explore more significant bioactive components of this plant.

1. Introduction

The genus *Garcinia* belonging to family Clusiaceae is used for the treatment of abdominal pain, suppuration, infections, leucorrhoea, ulcer and gonorrhea in folk medicine [1–4]. It is a rich source of prenylated xanthones and benzophenones, flavonoids and triterpenes which are reported to display significant antimicrobial, anti-inflammatory, anticancer and anti HIV activities [5–11]. Several studies have shown the cytotoxicity of benzophenones and triterpenes isolated from *Garcinia* genus [12,13]. For example, Yang et al. [14] reported the significant cytotoxic effect of benzophenones (guttiferones A and K) on HCT-11, HT-29 and SW-480 human colon cancer cell lines with IC_{50} ranging from 5 to 25 μM. Likewise, the study of Xu et al. [15] revealed the isolation of cytotoxic prenylated benzophenones (garciyunnanins A and B) against HeLa-C3 sensor cells and Elfita et al. [7] reported the cytotoxicity of a triterpene (3β-hydroxy-5-glutinen-28-oic acid) against MRC-5 cells isolated from *G. cymosa*.

G. hombroniana, a seashore mangosteen in Peninsular Malaysia is used to relieve itching and as a protective medicine against infections after childbirth [16]. The previous phytochemical investigation on pericarp, leaves and twigs of *G. hombroniana* showed the presence of xanthones, flavonoids and triterpenes [17–19] with significant LDL antioxidation and antiplatelet aggregation activities [20]. So far, to the best of the authors' knowledge, there is no authentic phytochemical and biological investigation on the bark and on the cytotoxic potential of the randomly isolated benzophenones and triterpenes from *G. hombroniana*. Taking this into consideration, the present study was carried out to investigate the bark of *G. hombroniana* for its bioactive chemical constituents. This paper describes the isolation, characterization, cytotoxic and antioxidant activities of the constituents **1**–**15** (Fig. 1).

2. Experimental

2.1. Plant materials

The plant materials were collected from Penang Botanical Garden, Penang. A voucher specimen (PBGK12) has been deposited at the herbarium of this Garden.

* Corresponding author. Fax: +60 46574854.
E-mail address: melati@usm.my (M. Khairuddean).

http://dx.doi.org/10.1016/j.bioorg.2014.04.003
0045-2068/

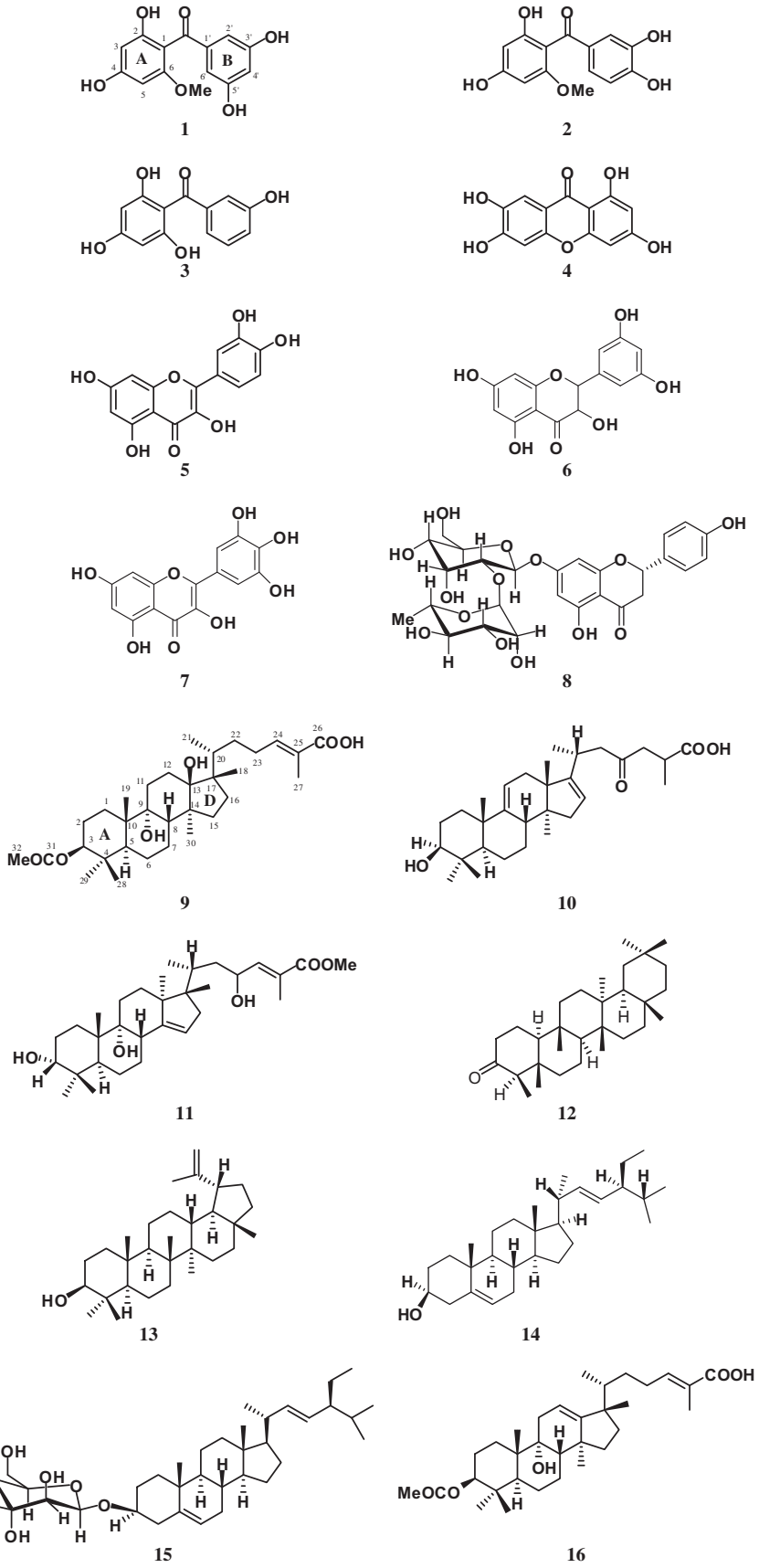

Fig. 1. Chemical structures of compounds **1**–**16**.

2.2. Chemicals and reagents

The chemicals of cytotoxic activity; DBTRG (glioma), MCF-7 (human breast cancer), U2OS (osteosarcoma) and PC-3 (prostate) cell lines were purchased from Sigma–Aldrich (USA). The chemicals of antioxidant activities; DPPH (2,2-diphenyl-1-picrylhydrazyl), ABTS (2,2′-azino-bis-3-ethyl benzthiazoline-6-sulphonic acid), TPTZ (2,4,6-tripyridyl-*s*-triazine), trolox and gallic acid were purchased from Sigma–Aldrich (Steinheim, Germany) and Merck (Darmstadt, Germany). All the solvents used in the extraction and isolation were of analytical grade.

2.3. Apparatus and instruments

Merck TLC plates (silica gel 60 F_{254}) were used to monitor the purity of compounds and visualized with a UV lamp (Vilber Lournet, multiband UV-254/356 nm), and/or by spraying with 95% methanolic H_2SO_4 and Libermann–Burchard's reagent followed by heating at 100–105 °C. Melting points were determined using a Stuart Scientific Melting Point SMP1 (UK). UV spectra were measured using a Perkin Elmer, Lambda 25 UV/Vis spectrometer. IR spectra were recorded in KBr using Perkin Elmer (USA) 2000 FT-IR spectrophotometer. The EI/ESI-MS analyses were carried out in the Mass Spectrometry Lab, National University Singapore (NUS). NMR experiments were performed using a Bruker Ascend 500 MHz (^{1}H) and 125 MHz (^{13}C) spectrometer (Bruker Biospin, Switzerland).

2.4. Extraction, isolation and purification

The air dried ground bark (5.2 kg) of *G. hombroniana* was sequentially extracted using Soxhlet extractor with *n*-hexane (C_6H_{14}), dichloromethane (DCM), chloroform ($CHCl_3$), ethyl acetate (EtOAc) and methanol (MeOH) at 40 °C. The filtered extracts were evaporated to dryness using a rotary evaporator at 40 °C to give a 30.1 g of *n*-hexane extract, 50.0 g dichloromethane extract, 5.0 g of a chloroform extract, 18.0 g of ethyl acetate extract and 30.1 g of a methanol extract.

An EtOAc extract (18.0 g) was chromatographed over silica gel using $CHCl_3$ as a packing solvent. The elution was carried out using $CHCl_3$ (100%), $CHCl_3$/EtOAc (9:1 to 0:10) and EtOAc/MeOH (9.5:0.5 to 8.5:1.5). Seven major combined fractions of the 42 sub-fractions were obtained and separated using silica gel CC. The sub fraction EFA6 (4.0 g) of yellow spots on TLC after treating with 5% methanolic H_2SO_4, was preceded to silica gel CC with solvent systems of $CHCl_3$, $CHCl_3$/Me_2CO and MeOH and fractions EFA6b1 to EFA6b35 were collected. Sub-fraction EFA6b2 which was further separated on CC, afforded compound **1** (120.0 mg) with 3:2 (v/v) $CHCl_3$/Me_2-CO. This was recrystalised from $CHCl_3$/MeOH (9:1). After further separation, the sub-fractions EFA6b10 to EFA6b12 yielded a yellow compound **4** in small yield with a solvent blend of $CHCl_3$/MeOH (8.5:1.5) on silica gel CC. Fractions EFA6b21 to EFA6b24 afforded compound **3** with EtOAc/MeOH (9:1). A combined fraction obtained by the CC of the sub-fractions EFA6b27 to EFA6b33 also gave a yellow spot accompanying by some other yellow components which on further silica gel CC with 100% $CHCl_3$ and a mixture of $CHCl_3$/MeOH gave compounds **2** and **8** when eluting with $CHCl_3$/MeOH (9:1 and 8:2), respectively.

A dried sub fraction EFA2 on dissolving in $CHCl_3$, gave a white precipitated solid which was found pure as compound **15** (30 mg) by TLC analysis as a single dark purple spot after treating with 95% methanolic H_2SO_4. The TLC analysis of fraction EFA4 (1.0 g) which showed few major yellow spots was chromatographed eluting with EtOAc/MeOH, afforded compounds **5**, **6** and **7**.

The DCM extract (17.0 g) was subjected to a series of silica gel CC purification and thoroughly eluted with a solvent systems of *n*-C_6H_{14}/EtOAc and EtOAc/MeOH in a polarity gradient manner (1:0, 9:1, 8:2, 7:3, 6:4, 1:1, 4:6, 3:7, 2:8 and 0:10 and finally flushed with methanol. Nine main fractions (DFB1 to DFB9) were obtained. Fraction DFB1 (4.0 g) was preceded for silica gel CC. Sub fractions, DSFBa6 to DSFBa8 collected with *n*-C_6H_{14}/EtOAc (8.0:2) were pure, combined and recrystalized from *n*-C_6H_{14}/MeOH (9.5:0.5) to give compound **12** (500 mg) in the form of white crystals. Fraction DFB2 (1.0 g) was applied to silica gel CC eluted with a mixture of *n*-C_6H_{14}/EtOAc in a polarity-gradient manner to give 15 fractions (DSFBb1 to DSFBb15). DSFBb7 to DSFBb10 with *n*-C_6H_{14}/EtOAc (8.5:1.5) were almost pure and afforded compound **14** (60.0 mg) on recrystallization from MeOH. Fraction DFB3 (180.0 mg) was rechromatographed with *n*-C_6H_{14}/EtOAc to give 10 sub-fractions DSFBc1 to DSFBc10. Sub-fractions DSFBc4 to DSFBc7 were combined and rechromatographed to afford compound **13** (20.0 mg). The fraction DFB7 (1.53 g) which showed three spots with purplish pink colour with Liebermann–Burchard's reagents was rechromatographed and eluted with a mixture of $CHCl_3$/EtOAc to give 30 fractions, DSFBe1 to DSFBe30. Sub-fractions DSFBe10 to DSFBe24 were combined again and eluted with EtOAc/MeOH (9:1) to yield compound **10** (50.0 mg) as a white precipitate while the filtrate upon drying afforded a semi-pure solid which was rechromatographed with EtOAc to yield compound **11** (7.0 mg) as a white amorphous solid. Fraction DFB8 (200.0 mg) was rechromatographed with *n*-C_6H_{14}/EtOAc and EtOAc/MeOH to give 35 sub-fractions of DSFBf1 to DSFBf35. Sub-fractions DSFBf17 to DSFBf25, showed a prominent purple spot on TLC plates which were combined and on further CC with *n*-C_6H_{14}/EtOAc and EtOAc/MeOH yielded a gummy white compound **9** (10.0 mg).

2.4.1. 2,3′,4,5′-tetrahydroxy-6-methoxybenzophenone (**1**)

Yellow crystals, mp: 243–246 °C; UV λ_{nm} ($\log\varepsilon$): 306 (3.66); IR (KBr) V cm^{-1}: 3545, 3300, 1635; ^{1}H and ^{13}C NMR: see Table 1; EI-MS 70 eV, *m/z* (rel. int.%): 276.1 $[M]^+$ (50) (calculated for $C_{14}H_{12}O_6$), 259 (55), 167 (77), 58 (41), and 43 (100).

2.4.2. 18(13 → 17)-abeo-3β-acetoxy-9α,13β-lanost-24E-en-26-oic acid (**9**)

White solid; mp: 128–130 °C; UV λ_{nm} ($\log\varepsilon$): 227 (4.13); IR (KBr) V cm^{-1}: 3461, 1710; ^{1}H and ^{13}C NMR: see Table 2; ESI-HR (positive mode): 555.30 $[M+Na]^+$ (100) (calculated for $C_{32}H_{52}O_6$-Na), 497 (30), 437 (95).

2.5. Cytotoxicity

The stock solutions of compounds **1** and **9** were prepared in the concentrations of 10, 20, 30, 50 and 75 μM in DMSO. MCF-7 and DBTRG cells were grown in the Roselle's Park Memorial Institute (RPMI) 1640 medium, U2OS cells in the Dulbecco's Modified Eagle's Medium (DMEM) and PC-3 in the Ham F12 K medium, all of which were supplemented with 10% of fetal bovine serum and 100 units/mL penicillin. The cells were maintained at 37 °C in a humidified condition, 5% of CO_2 in air and passage two to three times per week by light trypsinization. Control cells received the vehicle alone (<0.1%). A cytotoxicity detection kit was used to determine the cytotoxic effects of **1** and **9** on the aforementioned cell lines. This assay measures the amount of lactate dehydrogenase (LDH), a cytoplasmic enzyme, released by damaged cells into the cell culture supernatant post-treatment. Cells were seeded in 24-well plates at 100,000 cells per ml and were allowed to attach overnight to about 70% confluence. The medium was replaced with fresh medium containing 2% of fetal bovine serum prior to exposure of cells to **1** or **9** (10–75 μM) for up to 96 h. LDH assay was performed according to the manufacturer's instructions. The spectrophotometric absorbance of the colour generated was determined using a microplate reader at 490 and 620 nm referenced

Table 1
^{1}H, ^{1}H–^{1}H NOESY, ^{13}C and ^{1}H–^{13}C HMBC NMR data of **1** in MeOD-d_4.

S. No.	^{1}H		^{13}C	
	δ_H in ppm (multiplicity, J in Hz)	^{1}H–^{1}H NOESY	δ_C in ppm (C-Type)[a]	^{1}H–^{13}C HMBC
1			108.0 (C)	
2			162.7 (C)	
3	6.02 (*d*, 2.1, 1 H)	OMe	96.7 (CH)	C-1, C-2, C-4, C-5, C-6
4			162.8 (C)	
5	6.01 (*d*, 2.1, 1 H)	OMe	92.5 (CH)	C-1, C-3, C-4, C-6
6			164.6 (C)	
1′			144.1 (C)	
2′	6.59 (*d*, 2.0, 1 H)	OMe	107.9 (CH)	C-3′, C-4′, C-5′, CO
3′			159.3 (C)	
4′	6.45 (*t*, 2.0, 1 H)		107.1 (CH)	C-2′, C-3′, C-5′, C-6′
5′			159.3 (C)	
6′	6.59 (*d*, 2.0, 1 H)	OMe	107.9 (CH)	C-3′, C-4′, C-5′, CO
CO			199.8 (C)	
OMe	3.56 (*s*, 3 H)		56.0 (CH_3)	C-2, C-4

[a] C-Type was deduced from DEPT 135, 90 and Q NMR experiments.

Table 2
^{1}H, ^{13}C, ^{1}H–^{1}H COSY, NOESY and ^{1}H–^{13}C HMBC NMR data of **9** in MeOD-d_4.

No.	δ_H in ppm (multiplicity, J in Hz)		δ_C in ppm (C-type)[a]	^{1}H–^{1}H COSY	^{1}H–^{1}H NOESY	^{1}H–^{13}C HMBC
	Ha	Hb				
1[w]	2.01–1.97 (*m*)	1.63–1.62 (*m*)	29.8 (CH_2)	H2	H5, H7b	C3, C9, C10, C19
2[w]	1.65–1.64 (*m*)	1.53–1.49 (*m*)	24.7 (CH_2)	H1	Me19, Me28	C3, C4
3	4.46 (*dd*, 9.0, 7.0)		82.4 (CH)	H2	H5, Me29	C2, C4, C29, C31
4			38.6 (C)			
5	1.63–1.62 (*m*)		46.7 (CH)	H6	9OH, Me29, Me30	C4, C28, C29
6[x]	1.63–1.62 (*m*)	1.37–1.31 (*m*)	22.7 (CH_2)	H7		C5, C8, C9
7[x]	1.65–1.64 (*m*)	1.53–1.49 (*m*)	24.6 (CH_2)	H6		C5, C8, C9
8	1.48–1.40 (*m*)		46.8 (CH)		Me28	C6, C13, C14, C30
9			77.6 (C)			
10			44.2 (C)			
11[y]	1.77–1.73 (*m*)	1.48–1.40 (*m*)	29.7 (CH_2)	H12	9OH, Me30	C9, C13
12[y]	1.61–1.59 (*m*)		33.2 (CH_2)	H11		C9, C11, C17
13			84.7 (C)			
14			50.2 (C)			
15[z]	1.48–1.40 (*m*)		40.4 (CH_2)	H16	H15a with Me30	C13, C14, C17, C30
16[z]	1.61–1.59 (*m*)	1.26–1.25 (*m*)	38.1 (CH_2)	H15		C14, C17, C18, C30
17			52.8 (C)			
18	0.83 (*s*)		17.5 (CH_3)		H20	C13, C16, C17, C20
19	0.97 (*s*)		16.9 (CH_3)		H2a, Me28	C5, C9, C10
20	1.89–1.84 (*m*)		40.1 (CH)		Me18	C17, C18
21	0.87 (*s*)		15.5 (CH_3)		Me30	C17, C20, C22
22	1.89–1.84 (*m*)	0.97 (*s*)	33.1 (CH_2)	H23		C23, C24, C25, C26
23	2.26–2.21 (*m*)	2.19–2.11 (*m*)	28.6 (CH_2)	H24		C22, C24, C25
24	6.83 (*t*, 7.0)		145.0 (CH)	H23		C23, C26, C27
25			128.3 (C)			
26			172.0 (C)			
27	1.80 (*s*)		12.4 (CH_3)			C24, C25, C26
28	0.87 (*s*)		28.7 (CH_3)		H8	C29, C5, C29
29	0.89 (*s*)		17.0 (CH_3)		H5	C3, C28, C5
30	1.00 (*s*)		20.7 (CH_3)		Me21	C8, C13, C14
31			172.9 (C)			
32	2.02 (*s*)		21.2 (CH_3)		Me19	C3, C31

w, x, y and z represent intra and intercrossed correlations in ^{1}H–^{1}H COSY.
In ^{1}H–^{1}H NOESY data, ^{1}H–^{1}H COSY correlations are omitted.
[a] C-type was deduced from DEPT experiments.

wavelengths. The amount of LDH released was calculated according to the formula recommended in the manufacturer's protocol. As a control for maximum releasable LDH activity, cells were treated with a lysis reagent containing 1% of triton X-100 for 10 min while spontaneous LDH release was measured in the supernatant of untreated cultures. Additional cell-free wells containing assay medium alone were prepared for subtraction of absorption effects. This control provides information about the LDH activity present in the assay medium.

2.6. Antioxidant activities

Antioxidant activities of the compounds **1**–**15** were evaluated by free radical scavenging capacities using DPPH [21] and ABTS [22] and reducing power FRAP [21] assays. The compounds and the standard solutions of trolox and gallic acid were prepared in the concentration range of 1.0–50 μM. The inhibition percentage in DPPH and ABTS assays was calculated by the following formula.

$$\%\text{inhibition} = [(1 - (A_{\text{sample}}/A_{\text{control}})] \times 10$$

where A_{sample} is the absorbance of samples and $A_{control}$ is the absorbance of control. The results of DPPH and ABTS assays were expressed as IC_{50} values in μM and were calculated using GraphPad Prism 6.02 (GraphPad Software Inc., La Jolla, USA) while the reducing capacity of the compounds (FRAP) were expressed in μM trolox equivalent (μM TE).

2.7. Statistical analyses

All data were analyzed and expressed as means ± standard deviation of three replicates. The differences between the assayed values were analyzed using 1-way analysis of variance (ANOVA), followed by Tukey's HSD test at 95% and 99% confidence interval with SPSS software, version 19.0 (SPSS Inc. Chicago, USA). IC_{50} were calculated using GraphPad Prism 6.02 (GraphPad Software Inc. La Jolla, USA).

3. Results and discussion

3.1. Structure elucidation of isolated compounds

Compound 1 was obtained in the form of bright yellow crystals (the crystal structure data is already published [23] but the spectral data is new). The molecular formula was established as $C_{14}H_{12}O_6$ by EI-MS (Fig. S1, Sup. material), in which a molecular ion peak appeared at *m/z* 276.1. Both the UV (306 nm) and IR (1635 cm^{-1}) absorptions confirmed the presence of a conjugated keto group. In the ^1H NMR spectrum (Fig. S2, Sup. material), a doublet of two protons at δ_H 6.59 and a triplet of one proton at δ_H 6.45 with a *J* of 2.0 Hz, indicated *meta* coupling of three protons in one ring. In addition, two doublets at δ_H 6.02 and 6.01 observed were assigned to H-3 and H-5. The ^{13}C NMR spectrum (Fig. S3, Sup. material) displayed resonances of eight quaternary carbons, five methine carbons and one methoxy carbon which were deduced from DEPT 135, 90 and Q spectra (Fig. S4, Sup. material). The asymmetrical trisubstitution in ring A of **1** was confirmed by the signals at slightly different chemical shifts (δ_C 96.7 and δ_C 92.5) in the ^{13}C NMR, suggesting the location of CH_3O group at C-6 of ring A which differentiated it from its isomer; annulatophenone [24]. The ^1H–^{13}C HMQC spectrum (Fig. S5, Sup. material) helped in the assignment of the protonated carbons and ^1H–^{13}C HMBC spectrum (Fig. S6, Sup. material), confirmed the positions of the hydroxylated and methoxylated carbons. Furthermore, the position of the CH_3O group was confirmed by ^1H–^1H NOESY spectrum (Fig. S7, Sup. material), in which it displayed spatial coupling with protons at δ_H 6.02 which confirmed its substitution at C-6 in ring A. Based on these spectral data, **1** was identified as 2,3′,4,5′-tetrahydroxy-6-methoxybenzophenone. The complete assignment of the NMR spectroscopic data is given in Table 1.

Compound 9 was obtained as a white solid with a melting point of 156–159 °C. The EI-MS (Fig. S8(a), Sup. material) showed a molecular ion peak at *m/z* 514.5, suggesting a molecular formula of $C_{32}H_{50}O_5$ but it was realized from the ^{13}C and DEPT NMR data that the molecular mass at *m/z* 514.5 is due to the loss of a water molecule from the molecular ion, $[M-H_2O]^+$. However, the positive ESI-MS (see Fig. S8(b), Sup. material) showed a pseudo-molecular ion peak at *m/z* 555.30 $[M+Na]^+$, which suggested a molecular formula of $C_{32}H_{52}O_6$. The IR spectrum exhibited absorption bands at 3461 (O–H) and 1710 cm^{-1} (C=O) stretching frequencies, respectively. The ^1H NMR spectrum (Fig. S9, Sup. material and Table 2) showed signals of an olefinic proton at δ_H 6.83, an oxymethine proton at δ_H 4.46, and eight methyl groups at δ_H 2.02, 1.83, 1.0, 0.97, 0.89, 0.87 (2 × Me) and 0.83. The ^{13}C NMR spectrum (Fig. S10, Sup. material) exhibited signals of nine quaternary, five methine, 10 methylene and eight methyl carbons, deduced from DEPT 135, 90 and Q NMR spectra (Fig. S11, Sup. material).

These ^{13}C NMR data were similar to those of garcihombronane I acetate (**16**) [19] shown in Fig. 1, but with a difference of a hydroxylated quaternary carbon (C-13) in **9** instead of an unsaturated C-12 and C-13 in **16**. The disappearance of an olefinic proton and carbon at δ_H 5.17 and δ_C 115.5 in **16**, and the presence of an additional methylene (δ_C 33.2) and a hydroxylated quaternary carbon (δ_C 84.7) observed in the ^{13}C NMR spectrum of **9**, evidenced that **9** is a new garcihombronane with the same core structure of **16**. In ^1H–^1H COSY spectrum (Fig. S12, Sup. material, Table 2), correlations of an olefinic proton at δ_H 6.83 (H-24) with two non-equivalent protons at δ_H 2.26–2.21and 2.19–2.11 (H-23), correlations of H-23 with another pair of two non-equivalent protons at δ_H 1.89–1.84 and 0.97 (H-22), and a correlation of proton at δ_H 1.89–1.84 (H-20) with a singlet at δ_H 0.87 (Me-21) confirmed the presence of a double bond between C-24 and C-25 in a side chain of the type $CH(Me)CH_2CH_2CH{=}C(Me)COOH$. Direct connectivities of protons to the corresponding carbons were analyzed from ^1H–^{13}C HSQC spectrum (Fig. S13, Sup. material). The positions of the double bond Δ^{24-25}, COOH and the $OCOCH_3$ groups were determined by ^1H–^{13}C HMBC spectrum (Fig. S14, Sup. material and Table 2). The correlations of H-24 (δ_H 6.83) to C-26 (δ_C 172.0) and C-27 (δ_C 12.4) confirmed that the double bond is located between C-24 and C-25. A proton at δ_H 4.46 (H-3) demonstrated correlations with C-31 (δ_C 172.2), C-4 (δ_C 38.6), C-28 (δ_C 28.7) and C-29 (δ_C 17.5), and H-32 of the ester group showed correlations with C-31 and C-3, which along with the slight deshielded chemical shift of H-3 confirmed the position of $OCOCH_3$ group at C-3 (δ_C 82.4). Correlations of H-27 (δ_H 1.80) with C-26, C-24 (δ_C 145.0) and C-25 (δ_C 128.3) were observed which confirmed the position of a COOH group as C-26.

The relative configuration of **9** was established with the aid of ^1H–^1H NOESY spectrum (Fig. S15, Sup. material, Table 2), in which in the side chain, H-24 (δ_H 6.83) did not show any cross peak with Me-27 (δ_H 1.80). Thus the double bond at C-24/25 is *E*. The splitting pattern, coupling constant and a slightly downfield chemical shift (δ_H 4.46, *dd*, *J* = 9.0, 7.0 Hz) of H-3 indicated that H-3 and H-2 are diaxial with H-3α-oriented and the equatorial $OCOCH_3$ group is β-oriented. H-29 (δ_H 0.89) showed correlations with H-3 and H-5 (δ_H 1.63–1.62) which revealed that H-29, H-3 and H-5 are *cis* to one another. H-5 showed correlations with H-29, H-30 (δ_H 1.00) and a hydroxyl group (most probably 9–OH), which indicated that this OH is located at an α-axial position and all these protons are *cis*. Based on these NOESY results the relative configuration of **9** was established and identified as 18(13–17)-abeo-3β-acetoxy-9α,13β-lanost-24*E*-en-26-oic acid, a new naturally occurring triterpene, which was given a common name of Garcihombronane N.

Structures of the known constituents: **2** [25], **3** [26], **4** [27], **5** [28], **6** [29], **7**, **8**, **10**, **11** [19,20], **12** [30], **13** [31], **14** [32] and **15** [33] were identified by the measurements of 1D and 2D NMR spectroscopic data and comparison of their NMR data with those published in the literature.

3.2. Cytotoxicity

A cytotoxicity study was carried out on compounds **1** and **9**. The ability of **1** and **9** to induce cancer cell death was first tested on human cancer cell lines: DBTRG, PC-3, U2OS and MCF-7. Both compounds were found to be more toxic towards DBTRG cells as compared to other cancer cells. At 20 μM, these compounds induced maximum cell death of 49% and 24%, respectively after 72 h of treatment of the DBTRG cells. At the same concentration, **9** showed low cytotoxic effect on the U2OS cell line while **1** induced 27% cell death at 72 h but less than 10% cell death was observed for the PC-3 and MCF-7 cells when treated with either compound. However, a

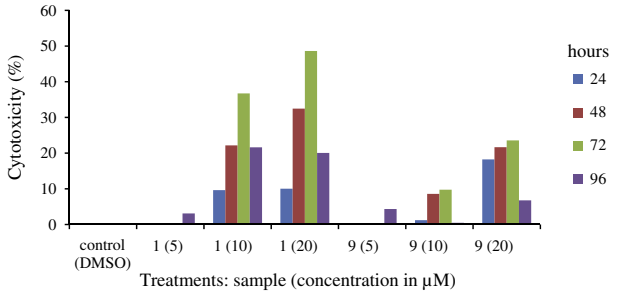

Fig. 2a. Cytotoxic effects of **1** and **9** on DBTRG cancer cell lines.

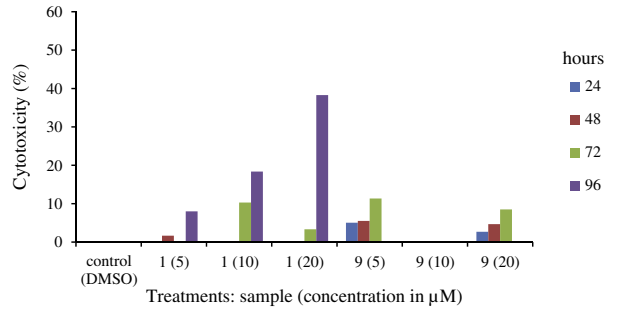

Fig. 2b. Cytotoxic effects of **1** and **9** on PC-3 cancer cell lines.

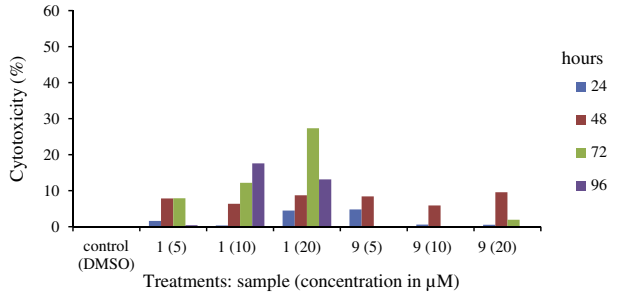

Fig. 2c. Cytotoxic effects of **1** and **9** on U2OS cancer cell lines.

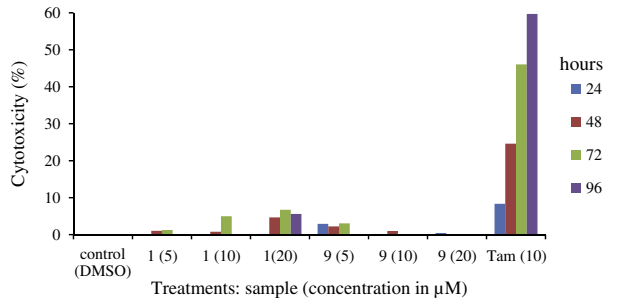

Fig. 2d. Cytotoxic effects of **1** and **9** on MCF-7 cancer cell lines.

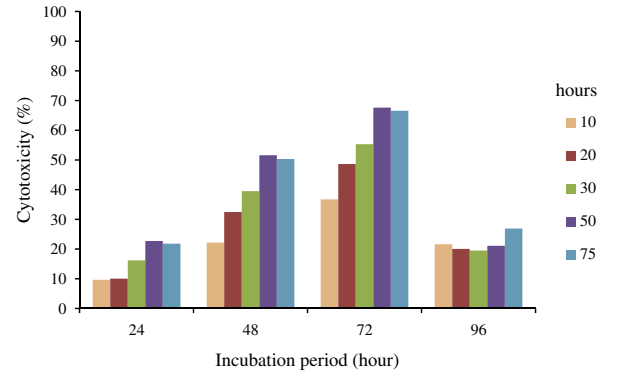

Fig. 3a. Dose- and time-dependent cytotoxic effects of **1** on DBTRG cells and EC_{50} determination.

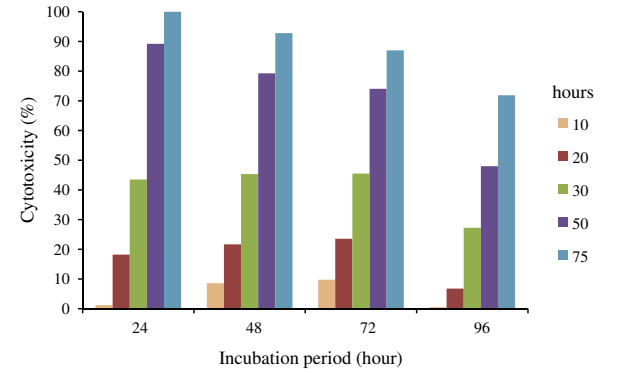

Fig. 3b. Dose- and time-dependent cytotoxic effects of **9** on DBTRG cells and EC_{50} determination.

higher level of cytotoxicity (38%) was seen after longer exposure (96 h) of PC-3 cells. The results as shown in Fig. 2a–2d hence, indicated that **1** and **9** have cytotoxic effects which are cell-line dependent. A dose–response analysis was also performed in order to determine the 50% effective concentrations (EC_{50}) of **1** and **9** on the DBTRG cells. Both **1** and **9** (10–75 μM for up to 96 h) were found to cause a time- and concentration-dependent cell death of the DBTRG cells. However, **9** has a higher cytotoxic potential with an EC_{50} of 34 μM as compared to that of **1** (EC_{50} of 48 μM) although **1** causes higher percentages of cell death at low concentrations as shown in Fig. 3a and 3b.

3.3. Antioxidant activities

Compounds **1**–**15** were also tested for *in vitro* antioxidant activities, in which only **1–8** showed potent radical scavenging capacities. In DPPH radical assay, **7** was the most active of all the phenolics with IC_{50} 3.89 μM, followed by **5**, **4** and **2** showing 50% inhibition at 4.78, 5.44 and 5.53 μM, respectively. Compounds **7**, **5**, **4** and **2** showed higher inhibition of DPPH than trolox (IC_{50} 23.7 μM) and gallic acid (IC_{50} 7.79 μM). In ABTS assay, except compounds **6** and **8**, all other compounds displayed higher inhibition of $ABTS^{\cdot+}$ than that of trolox (IC_{50} 10.9 μM). Compounds **1**, **2**, **4** and **5** inhibited $ABTS^{\cdot+}$ with the concentration comparable to gallic acid (IC_{50} 3.05 μM). The detailed IC_{50} of all the compounds and standards are listed in Table 3. The complete inhibition of the DPPH free radical by the compounds and trolox was attained at 30 and 50 μM except gallic acid (20 μM). On the other hand, all these compounds and trolox completely inhibited $ABTS^{\cdot+}$ at 30 μM except **3**, **6** and **8** which inhibited $ABTS^{\cdot+}$ at 50 μM. The DPPH and ABTS free radical inhibition profiles of **1**–**8** and the standards at various concentrations are shown in Fig. 4. In FRAP assay, among all the compounds, **7** showed the highest ferric ion reducing power with 326.5 ± 5.49 μM TE (Table 3). The free radical scavenging and the reducing activities of the phenolic compounds depend on number and location of hydroxyl group, stability in different system, O–H bond dissociation energy, resonance delocalization of the

Table 3
Antioxidant activities (IC_{50}, % inhibition) of compounds (**1**–**8**).

Compounds	DPPH assay		ABTS assay		FRAP assay μM TE
	(IC_{50})	Complete inhibition (%)	(IC_{50})	Complete inhibition (%)	
1	12.7 ± 0.33^{e}	86^{w}	4.92 ± 0.25^{b}	96^{y}	195.7 ± 1.68^{d}
2	5.53 ± 0.52^{c}	85^{v}	4.60 ± 0.32^{b}	92^{y}	255.3 ± 3.72^{e}
3	12.6 ± 0.81^{e}	87^{w}	9.9 ± 0.16^{c}	88^{y}	167.2 ± 4.65^{c}
4	5.44 ± 0.12^{c}	86^{v}	4.94 ± 0.43^{b}	89^{y}	268.2 ± 3.14^{f}
5	4.78 ± 0.15^{b}	89^{v}	4.17 ± 0.11^{b}	92^{y}	283.1 ± 3.74^{g}
6	13.5 ± 0.23^{f}	81^{w}	11.1 ± 0.79^{e}	88^{z}	128.7 ± 2.46^{b}
7	3.89 ± 0.07^{a}	92^{v}	3.72 ± 0.51^{a}	94^{y}	326.5 ± 5.49^{h}
8	28.1 ± 0.14^{h}	79^{w}	24.6 ± 0.37^{f}	84^{z}	89.63 ± 1.85^{a}
Trolox	23.7 ± 0.62^{g}	77^{w}	10.9 ± 0.18^{d}	99^{y}	–
Gallic acid	7.79 ± 0.05^{d}	94^{u}	3.0 ± 0.03^{a}	99^{x}	–

Results are mean values of 3 replicates ± SD.
Lowercase superscripts a, b, c, d, e, f, g, h represent significant differences at $p < 0.05$.
Lowercase superscripts u, v, w represents the complete inhibition at 20, 30 and 50 μM, respectively in DPPH radical scavenging assay.
Lowercase superscripts x, y, z represents the complete inhibition at 10, 30 and 50 μM, respectively in ABTS radical scavenging assay; The FRAP values are expressed as μM TE at 20 μM of the compounds.

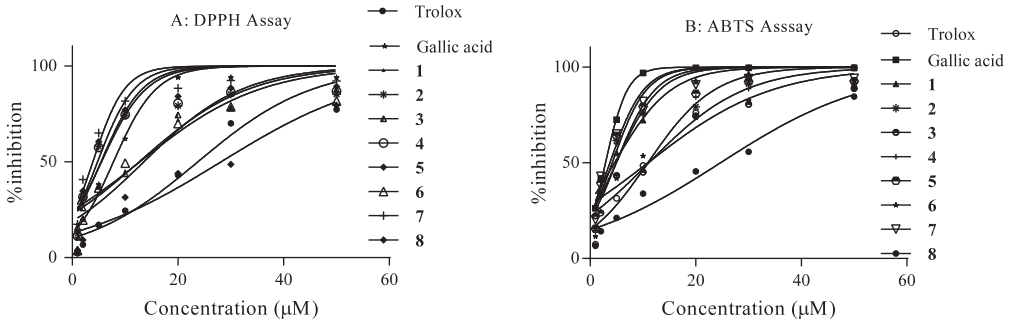

Fig. 4. (A) DPPH and (B) ABTS radical scavenging profiles of compounds (**1**–**8**) and standards (trolox and gallic acid) at different concentrations (1–50 μM).

antioxidant and steric hindrance [34]. In the present study, the DPPH assay for **1**–**8** was found linear with the number and position of the hydroxyl groups. However, in scavenging of ABTS radical, inhibition was found irregular to the number and position of the hydroxyl groups.

4. Conclusions

In the present study, benzophenones, flavonoids and triterpenes were isolated from the bark extracts of *G. hombroniana*. The isolated benzophenones and flavonoids from the ethyl acetate extract are reported for the first time from this species. This study also suggests the significant *in vitro* cytotoxic and antioxidant activities of the isolated phenolics. In view of the results from this study, it is concluded that the future phytochemical and pharmacological investigation on the bark of *G. hombroniana* using advanced experimental techniques could be of much importance.

Acknowledgments

The authors wish to acknowledge the Research University Grant (RU1001/PKIMIA/811129) provided by Universiti Sains Malaysia (USM). Nargis Jamila is thankful to TWAS and USM for the award of TWAS-USM PG fellowship.

Appendix A. Supplementary material

Supplementary data associated with this article can be found, in the online version, at http://dx.doi.org/10.1016/j.bioorg.2014.04.003.

References

[1] O.B. Balemba, Y. Bhattarai, C.S. Strahm, M.S.B. Lesakit, G.M. Mawe, Neurogastroenterol. Motil. 22 (2010) 1332–1339, http://dx.doi.org/10.1111/j1365-2982.01583.x.
[2] V.B. Braide, Fitoterapia LXIV (1993) 433–436.
[3] G.K. Jayaprakasha, P.S. Negi, B.S. Jena, Innov. Food Sci. Emerg. 7 (2006) 246–250, http://dx.doi.org/10.1016/j.ifset.2006.01.001.
[4] P. Moongkarndi, N. Kosem, S. Kaslunga, O. Luanratana, N. Pongpan, N. Neungton, J. Ethnopharmacol. 90 (2004) 161–166, http://dx.doi.org/10.1016/j.jep.2003.09.048.
[5] J. Ngoupayo, T.K. Tabopda, M.S. Ali, Bioorg. Med. Chem. 17 (2009) 5688–5695, http://dx.doi.org/10.1016/j.bmc.2009.06.009.
[6] L.J. Zhang, C.T. Chiou, J.J. Cheng, H.C. Huang, L.M.Y. Kuo, C.C. Liao, K.F. Bastow, K.H. Lee, Y.H. Kuo, J. Nat. Prod. 73 (2010) 557–562, http://dx.doi.org/10.1021/np900620y.
[7] E. Elfita, M. Muharni, M. Latief, D. Darwati, A. Widiyantoro, S. Supriyatna, H.H. Bahti, D. Dachriyanus, P. Cos, L. Maes, K. Foubert, S. Apers, L. Pieters, Phytochemistry 70 (2009) 907–912.
[8] V. Peres, T.J. Nagem, F. F de Oliveira, Phytochemistry 55 (2000) 683–710, http://dx.doi.org/10.1016/S0031-9422(00)00303-4.
[9] S. Tewtrakul, C. Wattanapiromsakul, W. Mahabusarakam, J. Ethnopharmacol. 121 (2009) 379–382, http://dx.doi.org/10.1016/j.jep.2008.11.007.
[10] Z.X. Xia, D.D. Zhang, S. Liang, Y.Z. Lao, H. Zhang, H.S. Tan, S.L. Chen, X.H. Wang, H.X. Xu, J. Nat. Prod. 75 (2012) 1459–1464, http://dx.doi.org/10.1021/np3003639.
[11] Q. Gu, R.R. Wang, X.M. Zhang, Y.H. Wang, Y.T. Zheng, J. Zhou, J.J. Chen, Planta Med. 73 (2007) 279–282, http://dx.doi.org/10.1055/s-2007-967113.
[12] H.D. Nguyen, B.T.D. Trinh, L.H.D. Nguyen, Phytochem. Lett. 4 (2011) 129–133, http://dx.doi.org/10.1016/j.phytol.2011.01.001.
[13] G.L. Pardo-Andreu, Y. Nunez-Figueredo, V.G. Tudella, O. Cuesta-Rubio, F.P. Rodrigues, C.R. Pestana, S.A. Uyemura, A.M.L. Leopodino, L.C. Alberici, C. Curti, Toxicol. Appl. Pharmacol. 253 (2011) 282–289, http://dx.doi.org/10.1016/j.taap.2011.04.011.
[14] H. Yang, M. Figueroa, S. To, S. Baggett, B. Jiang, M.J. Basile, I.B. Weinstein, E.J. Kennelly, J. Agric. Food Chem. 58 (2010) 4749–4755, http://dx.doi.org/10.1021/jf9046094.
[15] G. Xu, C. Feng, Y. Zhou, Q.B. Han, C.F. Qiao, S.X. Huang, D.C. Chang, Q.S. Zhao, K.Q. Luo, H.X. Xu, J. Agric. Food Chem. 56 (2008) 11144–11150, http://dx.doi.org/10.1021/jf802690g.

[16] M. Nazre, Gen. Resour. Crop Evol. 57 (2010) 1249–1259, http://dx.doi.org/10.1007/s10722-010-9588-y.
[17] S. Klaiklay, Y. Sukpondma, V. Rukachaisirikul, S. Phongpaichit, Phytochemistry 85 (2013) 161–166, http://dx.doi.org/10.1016/j.phytochem.2012.08.020.
[18] V. Rukachaisirikul, A. Adair, P. Dampawan, W.C. Taylor, P.C. Turner, Phytochemistry 55 (2000) 183–188, http://dx.doi.org/10.1016/S0031-9422(00)00191-6.
[19] V. Rukachaisirikul, S. Saelim, P. Karnsomchoke, S. Phongpaichit, J. Nat. Prod. 68 (2005) 1222–1225, http://dx.doi.org/10.1021/np050131j.
[20] F.C. Saputri, I. Jantan, Phytother. Res. 26 (2012) 1845–1850, http://dx.doi.org/10.1002/ptr.4667.
[21] K. Thaipong, U. Boonprakob, K. Crosby, L. Cisneros-Zevallos, D.H. Byrne, J. Food Compos. Anal. 19 (2006) 669–675, http://dx.doi.org/10.1016/j.jfca.2006.01.003.
[22] N. Jamila, M. Khairuddean, C.S. Lai, H. Osman, K.C. Wong, M. Vikneswaran, K.Y. Khaw, Afr. J. Pharm. Pharmacol. 28 (2013) 454–459, http://dx.doi.org/10.5897/AJPP12.944.
[23] N. Jamila, K.C. Wong, M. Khairuddean, S. Chantrapromma, H.K. Fun, Acta Crystallogr. E 67 (2011) o2717–o2718, http://dx.doi.org/10.1107/S1600536811037913.
[24] G.M. Kitanovo, P.T. Nedialkov, Phytochemistry 57 (2000) 1237–1243, http://dx.doi.org/10.1016/S0031-9422(01)00194-7.
[25] Y.M. Chiang, Y.H. Kuo, S. Oota, Y. Fukuyama, J. Nat. Prod. 66 (2003) 1070–1073, http://dx.doi.org/10.1021/np030065q.
[26] V.Y.M. Joong, G.H.L. Ee, M.A. Sukaria, Y. Hin, T. Yap, H.Y. Khong, M.K.Y. Chen, Res. J. Chem. Environ. 16 (2012) 36–39.
[27] N. Tadataka, U. Akira, M. Masako, H. Tsutomu, M. Toshio, K. Masanori, F. Seigu, Chem. Pharm. Bull. 32 (1984) 4455–4459.
[28] C.Y. Kim, H.J. Lee, M.K. Lee, M.J. Ahn, J. Kim, J. Sep. Sci. 30 (2007) 2693–2697, http://dx.doi.org/10.1002/jssc.200700168.
[29] S.Y. Kim, J.J. Gao, W.C. Lee, K.S. Ryu, K.R. Lee, Y.C. Kim, Arch. Pharmacal Res. 22 (1999) 81–85.
[30] D.M. de Oliveira de, W.daN. Mussel, L.P. Duarte, G.D.deF. Silva, H.A. Duarte, E.C.L. de Gomes, L. Guimaraes, S.A.V. Filho, Quím. Nova. 35 (2012) 1916–1921, http://dx.doi.org/10.1590/S0100-40422012001000005.
[31] D. Burns, W.F. Reynolds, G. Buchanan, P.B. Reese, R.G. Enriquez, Magn. Reson. Chem. 38 (2000) 488–493, http://dx.doi.org/10.1002/1097-458X200007.
[32] Y.C. Koay, K.C. Wong, H. Osman, I. Eldeen, M.Z. Aswami, Rec. Nat. Prod. 7 (2013) 59–64.
[33] M.S. Alam, N. Chopra, M. Ali, M. Niwa, Phytochemistry 41 (1996) 1197–1200, http://dx.doi.org/10.1016/0031-9422(95)00774-1.
[34] N. Nenadis, L.F. Wang, M. Tsimidou, H.Y. Zhang, J. Agric. Food Chem. 52 (2004) 4669–4674, http://dx.doi.org/10.1021/jf0400056.